

## RESEARCH ARTICLE

# Two isotypes of phosphatidylinositol 3-phosphate-binding sorting nexins play distinct roles in trogocytosis in *Entamoeba histolytica*

Natsuki Watanabe<sup>1,2,3</sup> | Kumiko Nakada-Tsukui<sup>2</sup>  | Tomoyoshi Nozaki<sup>3</sup> 

<sup>1</sup> Graduate School of Life and Environmental Sciences, University of Tsukuba, Tsukuba, Japan

<sup>2</sup> Department of Parasitology, National Institute of Infectious Diseases, Tokyo, Japan

<sup>3</sup> Department of Biomedical Chemistry, Graduate School of Medicine, The University of Tokyo, Tokyo, Japan

## Correspondence

Tomoyoshi Nozaki, Department of Biomedical Chemistry, Graduate School of Medicine, The University of Tokyo, 7-3-1 Hongo, Bunkyo-ku, Tokyo 113-0033, Japan.

Email: nozaki@m.u-tokyo.ac.jp

## Funding information

Japan Agency for Medical Research and Development, Grant/Award Numbers: JP18fk0108046, JP17jk0210018, 17fk0108122j1101, 18fk0108049j1102 and 19fk0108049j1103; Japan Society for the Promotion of Science, Grant/Award Numbers: JP26293093, JP17K19416, JP18H02650, JP16K08766, JP19H03463 and JP16H01210; Japan International Cooperation Agency; National Center for Global Health and Medicine Intramural Research Fund, Grant/Award Number: 29-2013; US-Japan Cooperative Medical Science Program

## Abstract

Phosphatidylinositol phosphates (PIPs) function as important second messengers in many cellular events. In the human intestinal protist *Entamoeba histolytica*, where phagocytosis/trogocytosis plays an indispensable role in proliferation and pathophysiology during infection, various PIPs are involved in multiple steps of phago/trogocytosis. PI3-phosphate (PI3P) plays a pivotal role in the biogenesis of phagosome/trogosomes via recruitment of PI3P effectors. Because no known PI3P downstream effectors are conserved in *E. histolytica*, we exploited a unique method to identify the proteins PI3P dependently recruited to phagosomes. We rationalised that overexpression of PI3P-binding GFP-HrsFYVE competes for PI3P on phagosomal membranes and results in dissociation of PI3P effectors from phagosomes. EhVps26 and EhVps35, but not sorting nexins (SNXs), of the retromer complex were detected from phagosomes only without GFP-HrsFYVE overexpression. Two potential SNXs, EhSNX1 and EhSNX2, identified in the genome, possess only phox homology domain and specifically bound to PI3P, but retromer components, EhVps26 and EhVps35, did not bind to PI3P. Live and immunofluorescence imaging showed that EhSNX1 was recruited to the trogocytic cup and tunnel-like structures, and subsequently, EhSNX2 was recruited to trogosomes. Furthermore, EhSNX1, but not EhSNX2, specifically bound to Arp2/3 and EhVps26, which were localised to the tunnel-like structures and the trogosomes, respectively. *EhSNX2* gene silencing increased trogocytosis, suggesting that EhSNX2 plays an inhibitory role in trogocytosis.

## KEYWORDS

pathogenesis, phagocytosis, phosphoinositide, trogocytosis, vesicular traffic

## 1 | INTRODUCTION

Phosphatidylinositol (PI) is one class of glycerophospholipids that is composed of an inositol ring, a phosphate, a glycerol skeleton, and

Natsuki Watanabe and Kumiko Nakada-Tsukui contributed equally to this paper.

This is an open access article under the terms of the Creative Commons Attribution-NonCommercial License, which permits use, distribution and reproduction in any medium, provided the original work is properly cited and is not used for commercial purposes.

© 2019 The Authors. Cellular Microbiology published by John Wiley & Sons Ltd.

two acyl chains. PI converts to seven types of phosphatidylinositol phosphates (PIPs): three types of PIP, three types of PIP<sub>2</sub>, and one PIP<sub>3</sub>. These seven different types of PIPs are localised on different cellular compartments and mediate a variety of the intracellular events by recruiting proteins possessing PIPs-recognizing domains such as FYVE (Fab1, YOTB1, Vac1, early endosomal antigen 1 [EEA1]), pleckstrin-homology, and phox homology (PX) domains. In mammalian cells, the forming phagocytic cup is partially decorated with PI(4,5)P<sub>2</sub> and PI(3,4,5)P<sub>3</sub>, and subsequently with PI3P as the phagosome encloses. Each PIP species recruits specific effector proteins to endosomes and phagosomes to promote formation and maturation. For example, PI3P recruits FYVE domain-containing EEA1, which is recruited to early endosomes and facilitates endosome maturation, whereas Rabenosyn-5, hepatocyte growth factor-regulated tyrosine kinase substrate (Hrs), and endosomal sorting complex required for transport (ESCRT) complex are also recruited to PI3P-rich membranes and play unique roles (Burman & Ktistakis, 2010).

*Entamoeba histolytica* is the protozoan parasite that displays inherited capacity of ingestion of foreign cells by phagocytosis and trogocytosis ("trogocytosis" means "nibble" or "chew" and thus, the word implies ingestion of live cells by pieces; Ralston, Solga, MacKey-Lawrence, Bhattacharya, & Petri, 2014) and responsible for human amebiasis causing an estimated 73,800 deaths annually (Lozano et al., 2012). Phagocytosis and trogocytosis have been implicated in self-defense, proliferation, and pathogenicity of this organism (Ralston, 2015; Ralston et al., 2014). In *E. histolytica*, it has been suggested that PI3P is involved in the early to late phases of phagocytosis/trogocytosis as it is localised on the phagocytic and trogocytic cup/the phagosome and trogosome (Nakada-Tsukui, Okada, Mitra, & Nozaki, 2009), whereas PI(3,4,5)P<sub>3</sub>, which is localised on the preclosed phagocytic and trogocytic cups and dissociated from them after sealing, in a relatively early phase (Byekova, Powell, Welter, & Temesvari, 2010). *E. histolytica* lacks an EEA1 homolog, but possesses 12 FYVE domain containing proteins (EhFPs, Nakada-Tsukui et al., 2009), 7 PX domain containing proteins, and 13 pleckstrin-homology domain containing proteins. However, the roles of these potential PIP-binding proteins in phagocytosis and trogocytosis remain elusive. We identified and characterised AGC kinases as PI(3,4,5)P<sub>3</sub>-binding proteins, which are involved in phagocytosis and trogocytosis. It has been shown that AGC kinase 1 is specifically involved in trogocytosis, whereas AGC kinase 2 is involved in both phagocytosis of dead mammalian cells and trogocytosis of live cells (Somlata, Nakada-Tsukui & Nozaki, 2017). Although PI(3,4,5)P<sub>3</sub> effectors have been in part characterised, the identity of PI3P effectors remains to be investigated because of the promiscuity of lipid-binding specificities of FYVE domain containing proteins, as shown for EhFP4, for instance.

In this study, we attempted to identify PI3P effectors recruited to phagosomes and trogosomes in a PI3P-dependent fashion by proteome analysis of purified phagosomes under PI3P-deprived (by overexpression of human HrsFYVE-GFP, using a tetracycline inducible system) and normal conditions. Finally, we proposed the model of how these sorting nexins (SNXs), the PI3P effectors, are involved in both positive and negative regulation of phagocytosis and trogocytosis.

## 2 | RESULTS

### 2.1 | Identification of retromer complex components as potential PI3P effectors that were recruited to phagosomes

To identify PI3P-binding effectors that are involved in the phagosome biogenesis, particularly on the late stage of maturation, in *E. histolytica* trophozoites, we opted to utilise differential proteomic analysis of the phagosomes under normal versus PI3P-deprived (competed) conditions. We rationalised that overexpression of a soluble PI3P-binding protein should compete for PI3P with other PI3P effectors that play a role in phagosome maturation to be recruited (Figure 1a). To this end, the *E. histolytica* strain that expresses GFP-fused HrsFYVE, which is the well-documented human PI3P-binding domain (Nakada-Tsukui et al., 2009) in a tetracycline-inducible fashion, was established. Expression of GFP-HrsFYVE in *E. histolytica* peaked at 24 hr of cultivation with 10 µg/ml of tetracycline (Figure S1). At this time point, we confirmed by immunofluorescence assay (IFA) that GFP-HrsFYVE was localised on the phagosomes containing human serum-coated Dynabeads (Figure 1b). We verified the purity of the phagosome-enriched fraction by the significant enrichment of GFP-HrsFYVE (Figure 1c) and the mature CP-A5 in the phagosome-enriched fraction. Altogether, these results suggest that our protocol of phagosome purification using serum-coated Dynabeads allowed us to successfully enrich phagosomes that were associated with GFP-HrsFYVE and thus PI3P, on phagosome membranes (Figure 1c). We isolated phagosomes using previously established protocols (Marion, Laurent, & Guillén, 2005) and analysed their proteome under the conditions of GFP-HrsFYVE being expressed and non-expressed. After all detected proteins were categorised by their functions, those detected at least two-fold higher under the GFP-HrsFYVE non-expressed condition compared with those under the GFP-HrsFYVE expressed condition were considered to be potential candidates of PI3P-binding proteins (Table S1). Only proteins categorised to lipid metabolism and vesicular trafficking are shown in Figure 1d. Among them, vacuolar protein sorting (Vps) 26 and Vps35, both of which are the components of the retromer complex, were detected, which were mainly investigated in this study, whereas analysis of other components will be described elsewhere.

### 2.2 | In silico identification of SNXs in *E. histolytica*

In mammalian cells, the retromer complex is known to be involved in recycling of transmembrane receptors from endosomes to the trans-Golgi network (Bonifacino & Hurley, 2008). It has been demonstrated that the retromer complex consists of two subcomplexes: the major subcomplex of Vps26/Vps29/Vps35 and a combination of SNX1 or 2, SNX5 or 6, and SNX3. The retromer is recruited to PI3P-rich endosomes via PX domain of SNX3 (Seaman, 2012). The components of the major subcomplex (Vps26/Vps29/Vps35) have been identified and investigated in *E. histolytica* (Nakada-Tsukui, et al., 2005; Picazzari et al., 2015; Srivastava et al., 2017).

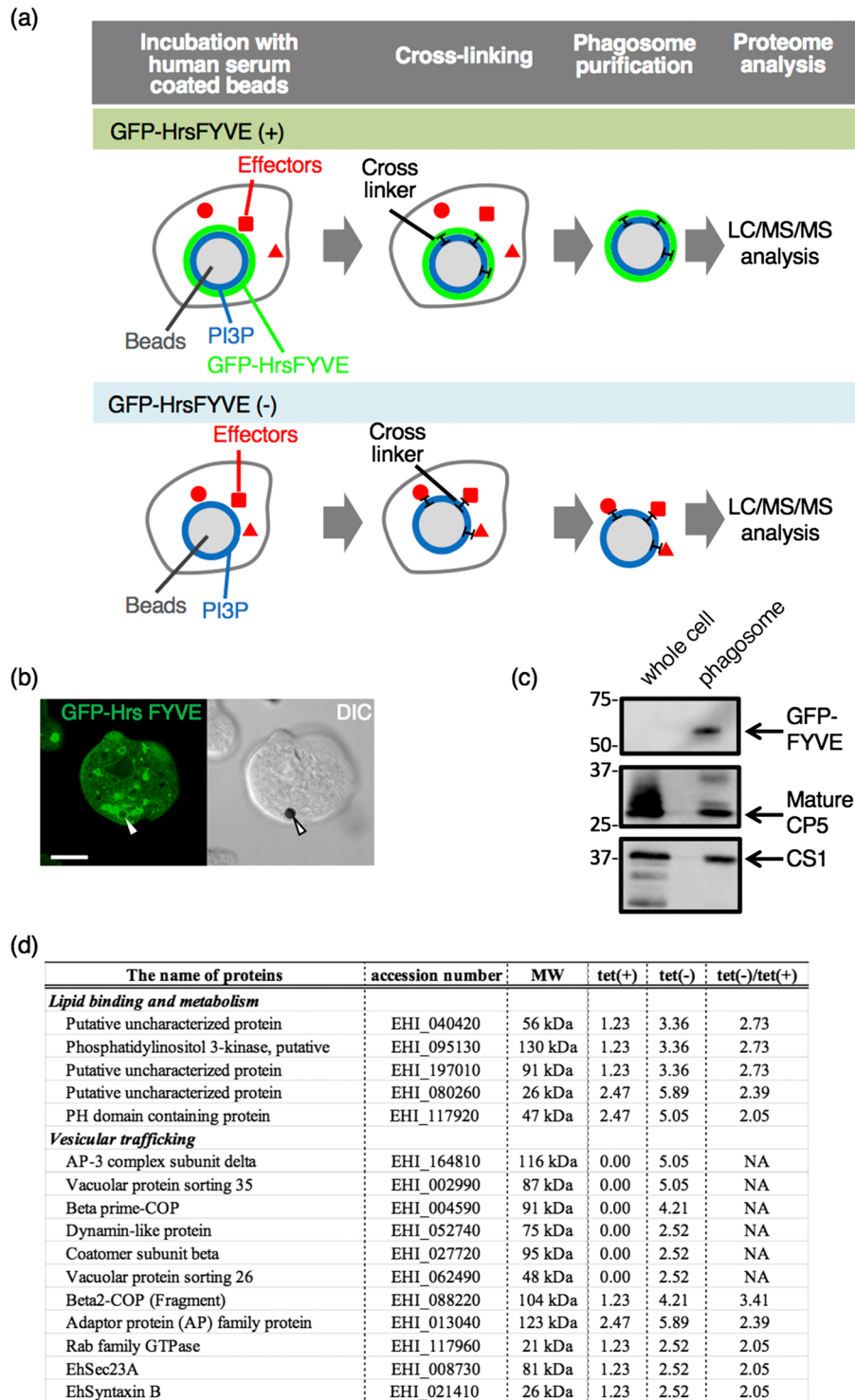


**FIGURE 1** Identification of PI3P-binding effector proteins involved in phagosome biogenesis. (a) The strategy and rationale used in this study to identify PI3P-binding effector proteins involved in phagosome biogenesis. See text for details. (b) Verification of the recruitment of GFP-HrsFYVE to phagosomes by fluorescence microscopy. The *Entamoeba histolytica* transformant cells that expressed GFP-HrsFYVE under tetracycline induction were cultured in the presence of 10  $\mu\text{g}/\text{ml}$  of tetracycline for 24 hr and then incubated with human serum-coated beads for 30 min. Arrowheads indicate ingested beads. (c) Validation of the recruitment of GFP-HrsFYVE to phagosomes by phagosome purification followed by immunoblot analysis. The bead-containing phagosomes were purified as described in Section 4 and subjected to SDS-PAGE and immunoblot analyses. GFP-HrsFYVE and mature CP-A5 were detected with anti-myc, anti-GFP, and anti-CP-A5 antibody, respectively. (d) The categorised list of proteins that are differentially excluded from phagosomes in GFP-HrsFYVE-dependent fashion. Tet(+) and tet(-) indicate the conditions where GFP-HrsFYVE expression was induced with 10  $\mu\text{g}/\text{ml}$  of tetracycline or not induced. The values indicate the relative frequency of the detected peptides corresponding to each protein. "tet(-)/tet(+)" indicates the division of the value of tet(-) by the value of tet(+). A whole list of the detected proteins from purified phagosomes are found in Table S1



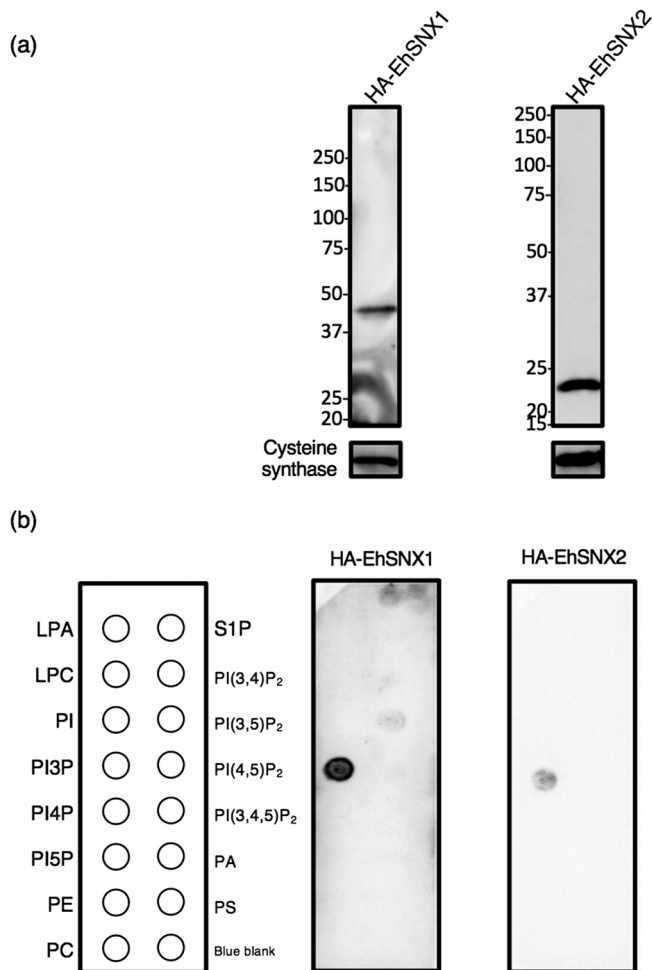


**FIGURE 3** Lipid-binding specificity of EhSNX1 and EhSNX2. (a) Verification of the expression of EhSNX1 and EhSNX2 in HA-EhSNX1- and HA-EhSNX2-expressing transformants by immunoblotting using anti-HA antibody. Approximately 20  $\mu$ g of total lysates from these strains were loaded. Cysteine synthase 1 was detected by anti-CS1 antiserum as a loading control. (b) Lipid-binding specificity of EhSNX1 and EhSNX2 observed by lipid overlay assay. A panel of PIPs and phospholipids spotted on nitrocellulose membrane was incubated with total lysates from HA-EhSNX1- and HA-EhSNX2-expressing transformants. The membranes were reacted with anti-HA antibody. LPA, lysophosphatidic acid; LPC, lysophosphocholine; PA, phosphatidic acid; PC, phosphatidylcholine; PE, phosphatidylethanolamine; PS, phosphatidylserine; S1P, sphingosine-1-phosphate

was closed (data not shown, see below for live imaging quantitation). Unlike EhSNX1, EhSNX2 was seldom present on the preclosure trogocytic cup, but localised on the closed trogosomes associated with EhVps26 (Figure 4b).

## 2.5 | Live imaging and quantification of GFP-EhSNX1/2 during trogocytosis

We monitored (Movies S1 and S2) and quantified (Figure 5) GFP-EhSNX1/2 on the trogocytic cup (and tunnel-like structures) and the trogosome during trogocytosis, according to the protocol described in

Section 4. GFP-EhSNX1 was recruited to the trogocytic cup when the cup was formed and remained associated until 108 s (note that the movie started to be recorded 4–7 s after adherence; Movie S2, Figure 5). The intensity of GFP-EhSNX1 was detected after the attachment of the trophozoite to the CHO cell and gradually decreased during trogosome maturation. On the contrary, GFP-EhSNX2 was recruited to the trogosome after the trogocytic cup was enclosed (Movie S2). The signal of GFP-EhSNX2 remained low until 108 s; it suddenly increased at 124 s (Figure 5). This live imaging suggests sequential processes in which GFP-EhSNX2 recruitment to the trogosome occurred after GFP-EhSNX1 dissociation from the trogosome.

## 2.6 | Interaction between EhSNX1 and the retromer complex demonstrated by immunoprecipitation

To demonstrate physical interaction between EhSNX1/2 and EhVps26 containing the retromer complex during trogocytosis, immunoprecipitation was performed with anti-EhVps26 antiserum using lysates from EhSNX1-HA expressing cells. Expression of EhSNX1-HA was confirmed by immunoblot analysis using anti-HA antibody (Figure 6a). For unknown reasons, EhSNX2-HA-expressing transformant could not be established (data not shown), and HA-EhSNX2 was used as control. Because EhSNX1 was found on the trogocytic cup/trogosome during trogocytosis of CHO cells, EhSNX1-HA-expressing cells were coincubated with CHO cells for 30 min and then, subjected to immunoprecipitation with anti-EhVps26 antiserum, followed by immunoblot analysis using anti-HA antibody, anti-EhVps26, and anti-EhVps35 antisera. EhVps26, EhVps35, and, in a lesser amount, EhSNX1-HA were immunoprecipitated from EhSNX1-HA-expressing cells (Figure 6b). HA-EhSNX2 was not coprecipitated with EhVps26, suggesting that the interaction with EhVps26 was specific to EhSNX1, but not EhSNX2.

## 2.7 | Interaction between Arp 2/3 complex component and EhSNX1 demonstrated by immunoprecipitation

To further understand the role of EhSNX1, immunoprecipitation was performed using the strain expressing EhSNX1 with the amino-terminal HA. HA-EhSNX1 was precipitated with anti-HA agarose after co-incubation with CHO cells for 30 min. One specific band around 20 kDa was detected after SDS-PAGE and silver staining (Figure 7a) and subjected to mass spectrometry analysis (Figure 7b). Notably, two of eight detected proteins (EHI\_174910; EHI\_030820) were C3 and C4 components of actin-related protein (Arp) 2/3 complex. To verify the interaction, the strain expressing FLAG-tagged 2/3 complex subunit 3 (EhArpC3; FLAG-EhArpC3) was established. The FLAG-EhArpC3 localisation was examined by IFA using anti-FLAG antibody. FLAG-EhArpC3 was localised on the tunnel-like structure (corresponding to the neck of a flask) during trogocytosis of CHO cells (Figure 7c). On the other hand, EhVps26 was never found on the tunnel-like structure, but on the bottom region of the trogocytic cup (before closure) and on the trogosome (after closure).

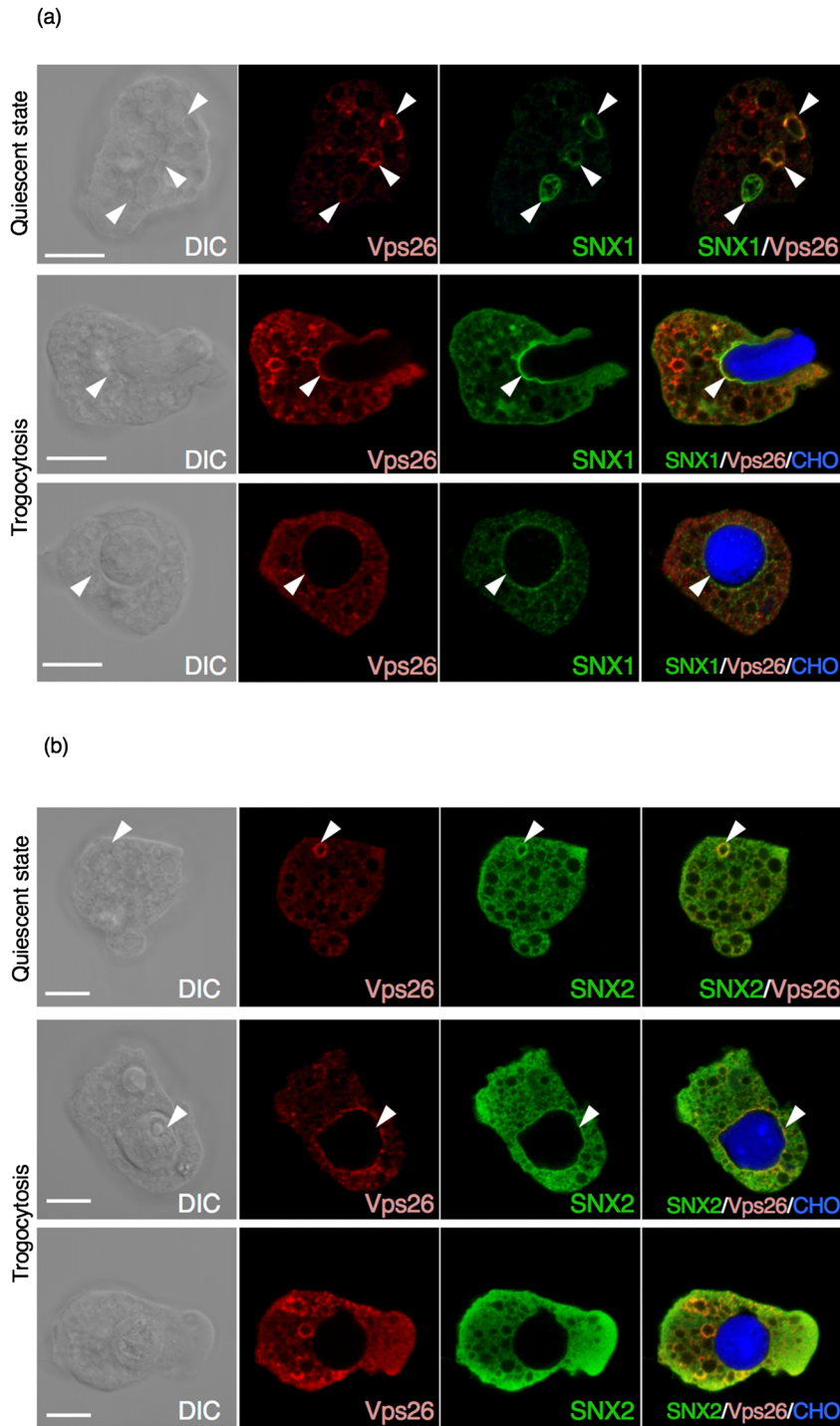


**FIGURE 4** Localisation of HA-EhSNX1 and HA-EhSNX2. Localisation of EhSNX1 and EhSNX2 (a, b) was examined by immunofluorescence assay in quiescent state and during phagocytosis. HA-EhSNX1/2 and EhVps26 were detected by anti-HA antibody and anti-EhVps26 antiserum, respectively. HA-EhSNX1/2 are shown in green, EhVps26 in red, and Chinese hamster ovary (CHO) cells were stained by CellTracker Blue. Differential interference contrast (DIC) and fluorescence images are shown. Scale bars are 10  $\mu$ m. Upper panels, in quiescent state; middle panels, during internalisation of a CHO cell (a), after closure of the trogosome (b); lower panels, after closure of the trogosome. Arrowheads depict vesicles, vacuoles, phagosomes, and the phagocytic cup where EhSNX1 or 2 is colocalised with EhVps26

## 2.8 | Transcriptional gene silencing of *EhSNX1* gene reduced recruitment of EhVps26 to the trogosome, whereas that of *EhSNX2* gene upregulated trogocytosis

To better understand how EhSNXs are involved in trogocytosis and phagocytosis, we performed transcriptional gene silencing (gs) of *EhSNX1* and *EhSNX2* genes. In the parental G3 line transformed with the mock vector, the level of *EhSNX2* mRNA is approximately 3.0-fold higher than that of *EhSNX1*. The level of *EhSNX1* transcript was reduced by 81 % by *EhSNX1* gene silencing, whereas that of *EhSNX2*

was conversely increased by 41 % (Figure 8a). In contrast, the level of *EhSNX1* and *EhSNX2* transcripts was reduced by 55 % and 94 % by *EhSNX2*, respectively (Figure 8a).

Because EhSNX1 physically interacts with the major retromer subcomplex (see above), gene silencing of *EhSNXs* can potentially affect localisation of the complex during trogocytosis and phagocytosis and also efficiency of ingestion. EhVps26 was swiftly recruited, together with EhSNX1, to the trogocytic cup during trogocytosis of CHO cell (Figure 4a). Almost all (96%) of CHO cell-containing trogosomes in the control strain were decorated with EhVps26 at 10

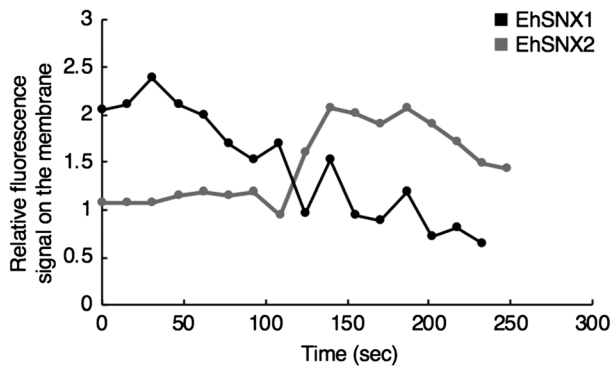


**FIGURE 5** Kinetics of association of GFP-EhSNX1/2 to the trophosome membrane during Chinese hamster ovary (CHO) cell internalisation. Fluorescence intensity of GFP-EhSNX1/2 on the trophosome membrane relative to the cytoplasm was monitored during trogocytosis of CHO cells. The images started to be collected 4–7 s after the initiation of the trogocytic cup formation, and this timing was set to zero. Y-axis represents the mean fluorescence signal per pixel of GFP-SNX1/2 on the trophosome membrane relative to that in the cytosol. One representative image each of three independent experiments is shown. Only representative movies were analysed, but other movies also showed similar kinetics

min of co-incubation with CHO cells (Figure 8b). At 30 min, a slightly less proportion (81%) of trophosomes in the control were still decorated with EhVps26. Although statistically insignificant ( $p$  value .44 and .11, at 10 and 30 min, respectively), gene silencing of *EhSNX1* caused less

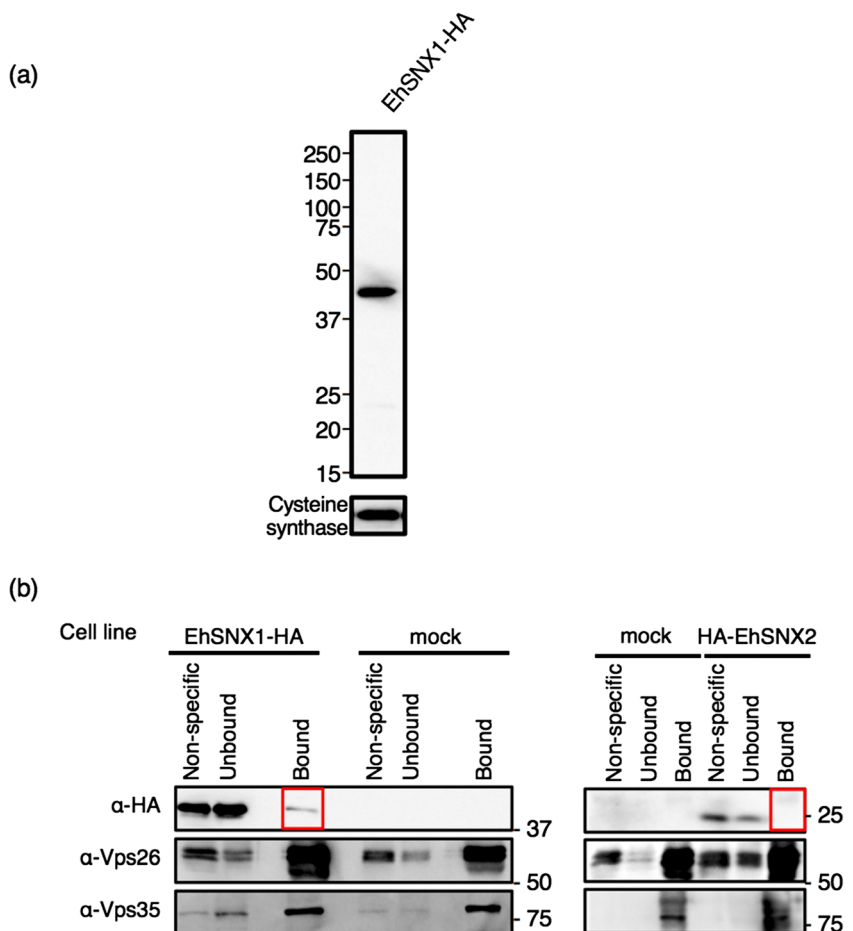
recruitment of EhVps26 to trophosomes compared with the control (4% and 14% reduction compared with the control at 10 and 30 min, respectively). Gene silencing of *EhSNX2* caused no change in the association of EhVps26 with trophosomes at 10 and 30 min. Next, we measured the total volume of ingested CHO cells per trophozoite, in EhSNX1gs, EhSNX2gs, and mock strains, on image cytometer CQ1 to estimate the efficiency of trogocytosis. The amoebic transformants were cultivated with CHO cells, and images were captured every 10 min for 80 min. Interestingly, trogocytosis significantly increased by 1.4- to 2.0-fold in EhSNX2gs strain compared with the control at all time points ( $p < .05$ ; Figure 8c). On the other hand, the volume of ingested CHO cells was not changed in EhSNX1gs strain at any time point. Phagocytosis was also affected by *EhSNX2* gene silencing; the volume of ingested pre-killed CHO cells increased by 1.4- to 2.0-fold in EhSNX2gs strain at all time points, similar to the effects on trogocytosis (Figure S4).

### 3 | DISCUSSION

#### 3.1 | EhSNX1/2 are downstream effectors of PI3P signals on the trophosome membrane

PIPs-mediated signalling plays a pivotal role in phagocytosis and trogocytosis in *E. histolytica*. In this study, we identified for the first

**FIGURE 6** Binding of EhSNX1 with the retromer complex. (a) Verification of the expression of EhSNX1-HA by immunoblot analysis using anti-HA antibody. Approximately 20  $\mu$ g of total lysates from these strains were loaded. Cysteine synthase 1 was detected by anti-CS1 antiserum as a loading control. (b) Immunoprecipitation of EhVps26 and EhSNX1-HA followed by immunoblot analysis. After 30 min co-culture with EhSNX1-HA, HA-EhSNX2, or mock transformant cells with CHO cells, the amoebae were collected to produce lysates, which were subjected to immunoprecipitation by anti-Vps26 antiserum. The immunoprecipitated ("Bound"), unbound supernatant ("Unbound"), and non-specific (protein G-Sepharose control beads that were preincubated with lysates, washed, and boiled with SDS loading buffer) fractions were analysed with SDS-PAGE and immunoblot analyses using anti-HA antibody, anti-Vps26, and anti-Vps35 antisera



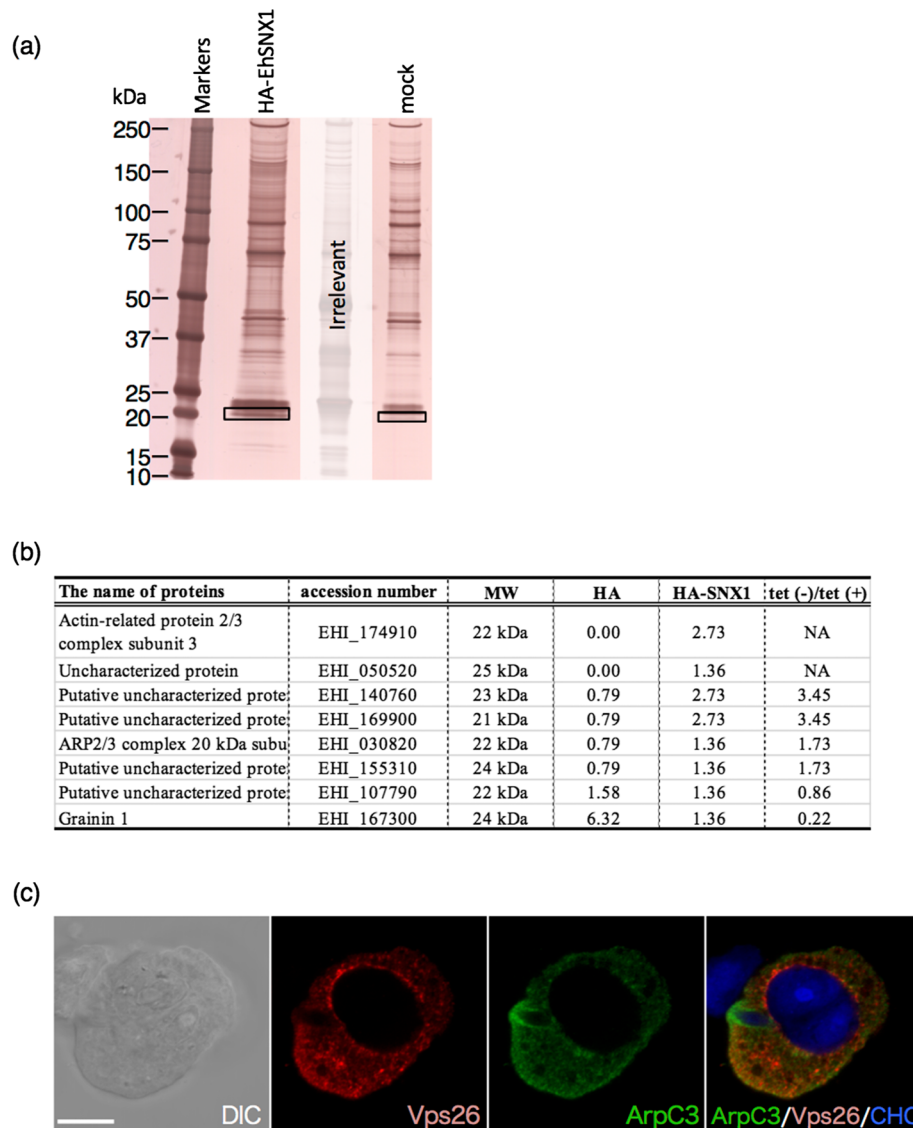


**FIGURE 7** Identification of candidate binding proteins of EhSNX1. (a) Silver-stained SDS-PAGE gel of the immunoprecipitated samples from HA-EhSNX1 and mock transformants using anti-HA antibody. The rectangles indicate the region of the specific band excised from HA-EhSNX1 and its corresponding region from control. (b) The proteins that were detected from the unique band specifically recognised from HA-EhSNX1-expressing transformants by immunoprecipitation using anti-HA antibody. Proteins that were not detected from the HA-EhSNX1 are excluded from the table. The values indicate the relative frequency of the detected peptides corresponding to each protein. “HA-EhSNX1/HA” indicates the division of the value of HA-EhSNX1 by the value of HA control. A whole list of the detected proteins is found in Table S2. (c) The localisation of EhArpC3 and EhVps26 during trogocytosis. FLAG-EhArpC3 transformant was co-cultured with CHO cells stained with CellTracker Blue for 15 min. FLAG-EhArpC3 and EhVps26 were detected using anti-FLAG antibody and anti-EhVps26 antiserum, respectively. FLAG-EhArpC3 is shown in green; EhVps26 is shown in red. Scale bar is 10  $\mu$ m

time the retromer complex, in particular SNXs, as a PI3P downstream effector on the phagosome and trogosome membrane in *E. histolytica*. It has been well established that in mammalian cells, PI3P is recruited to phagosomes and trogosomes after complete closure of the phagocytic/trogocytic cup and formation of the phagosome/trogosome, and that PI3P effectors such as EEA1 is recruited to the enclosed phagosomes to facilitate maturation of phagosome/trogosomes. It has been shown in *E. histolytica* that PI3P is localised on the phagocytic cup before closure as well as on the enclosed phagosomes (Nakada-Tsukui et al., 2009), and the timing of PI3P recruitment to the phagocytic and trogocytic cup in *E. histolytica*

appears to be different from human cells (Yeung & Sergio, 2007). However, as no known PI3P effector homologs were found in the *E. histolytica* genome, the role of PI3P on the phagocytic/trogocytic cup and phagosome/trogosome and its downstream effectors remained elusive. To identify the proteins that are recruited to phagosomes in a PI3P-dependent manner, we took a unique approach using our unique reverse genetic system in which PI3P-binding Hrs-FYVE domain fused with GFP, expressed in a tetracycline-inducible manner, competes with endogenous PI3P binding proteins for PI3P on phagosome and trogosomes. Because such interaction between PI3P and its effectors is transient and unstable, we needed to use a

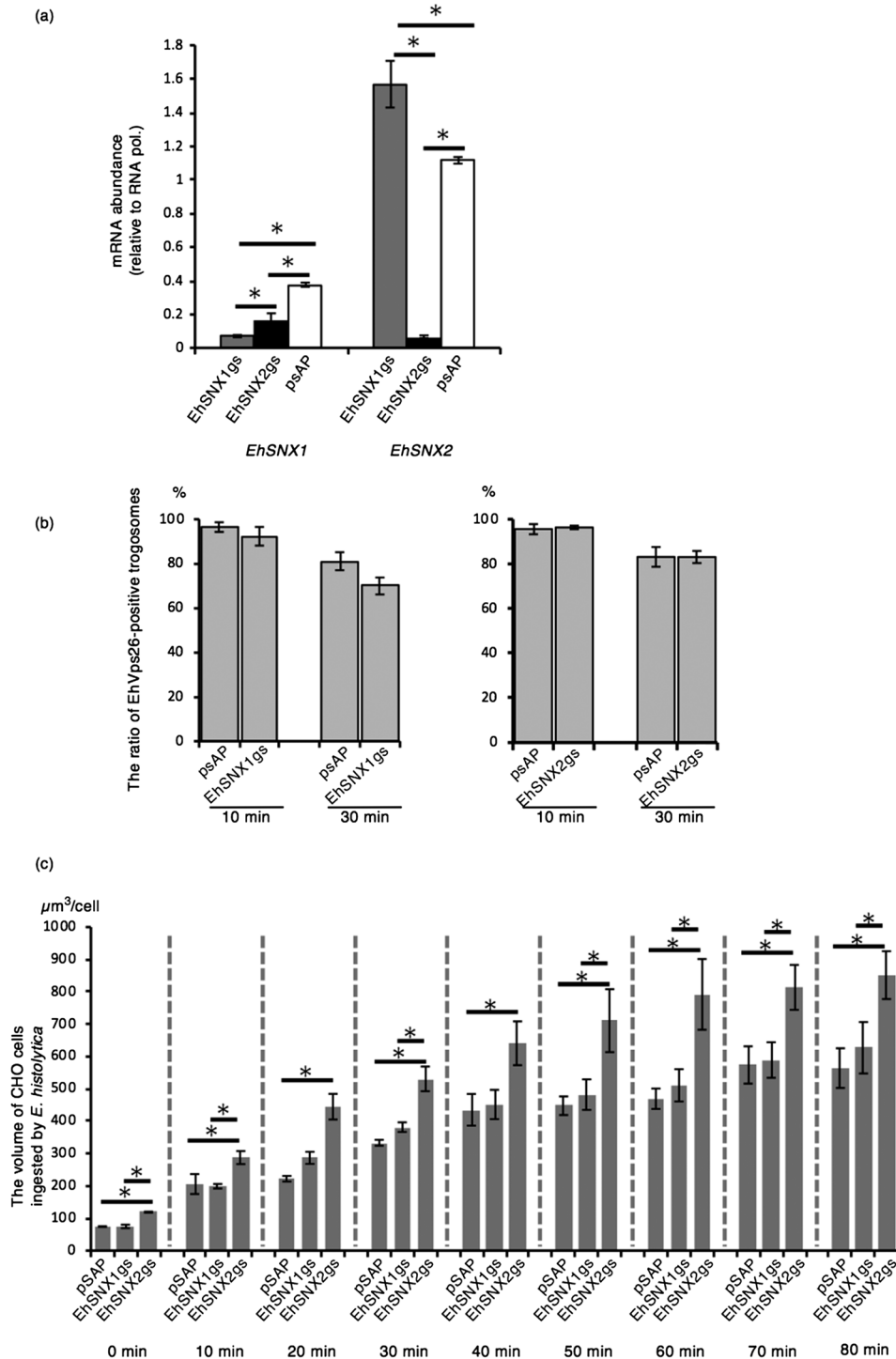


**FIGURE 8** The effect of gene silencing of *EhSNX1* and *EhSNX2* on the retromer recruitment to trogosomes and trogocytosis. (a) The levels of *EhSNX1* and *EhSNX2* transcripts in *EhSNX1gs*, *EhSNX2gs*, and control strains. The transcript levels are shown relative to that of RNA polymerase II. (b) The effects of gene silencing of *EhSNX1* and *EhSNX2* on the recruitment of EhVps26 to trogosomes. Trophozoites were allowed to ingest live Chinese hamster ovary (CHO) cells for 10 or 30 min and subjected to immunofluorescence assay. Images of trophozoites that had ingested CHO cells were randomly captured, and the number of all trogosomes and Vps26-positive trogosomes were counted to estimate the ratio of Vps26-positive trogosomes. (c) The effects of gene silencing of *EhSNX1* and *EhSNX2* genes on trogocytosis. Trophozoites of *EhSNX1gs* and *EhSNX2gs* strains stained with CellTracker Green were incubated with CHO cells stained with CellTracker Blue as described in Section 4. The images were taken on CQ1 every 10 min for 80 min. The volume of the ingested CHO cells (blue) was calculated using three-dimensionally reconstituted data. Bars indicate standard errors. Asterisks indicate statistical significance by Tukey test ( $p < .05$ ). Experiments were conducted three times independently, and a representative data set is shown

cross-linker and a phosphatase inhibitor to immobilise such interaction (Figure S2).

SNXs were not identified from *E. histolytica* in our previous study by biochemical approaches (Nakada-Tsukui et al., 2005). Furthermore, an in silico gene survey also failed to identify SNX homologs (Nakada-Tsukui et al., 2005), which was likely due to our using of yeast Vps5p as a query for Blastp search. *E. histolytica* SNXs were identified when human SNX1 or SNX3 was used as a query, but not by using PX domain from other protein as a query (the E-values of the Blastp search using HsSNX1 or HsSNX3 as a query were 4e-6 and 5e-10 for EHI\_060320, respectively; 1e-04 and 3e-13 for EHI\_004400; whereas that using yeast Vps5p was 0.007 for EHI\_060320 and 0.002 for EHI\_004400).

### 3.2 | PIP specificity of EhSNX1/2 and human SNXs

The PIP specificity of EhSNX1 and EhSNX2 compared with that of human SNX1-3 is intriguing. In humans, there are >30 members of SNXs known (Cullen, 2008) containing only several members with known PIP specificity. Human SNX1 and SNX2 showed preference in the order of PI(3,4,5)P<sub>3</sub>>PI(3,5)P<sub>2</sub>>PI3P and PI3P>PI4P>PI5P, respectively, whereas human SNX3 almost exclusively binds to PI3P, similar to EhSNX1 and EhSNX2 (Worby & Dixon, 2002). Amino acid alignment shows six amino acid residues that are shared by EhSNX1, EhSNX2, and HsSNX3, but not conserved in both HsSNX1 and HsSNX2, including EhSNX1 T107 of (EhSNX2 T28), EhSNX1 Y131 (EhSNX2 Y53), EhSNX1 L160 (EhSNX2 L82), EhSNX1 G162 (EhSNX2 G84), EhSNX1 F175 (EhSNX2 F96), and EhSNX1 I191 (EhSNX2 I112; Figure S3). The conservation of EhSNX1 G162 (EhSNX2 G84) corresponding to HsSNX3 G94 is of particular interest as these residues are also exclusively present in HsSNX11-13 and 27 (Lenoir et al., 2018), among which PIP specificity of only HsSNX13 was shown: preferred binding to PI3P and PI5P over PI(3,5)P<sub>2</sub> and PI4P (Worby & Dixon, 2002). These data suggest that EhSNX1 G162 (EhSNX2 G84) potentially contributes to PI3P specificity. Although PIP specificity may be affected by other domains than PX for the proteins that contain multiple domains such as HsSNX13 (Cullen, 2008), those of EhSNX1 and EhSNX2 are likely to be attributable to only the PX domain, similar to HsSNX3.

### 3.3 | EhSNX1 and EhSNX2 have different roles during trogocytosis

Two SNXs from *E. histolytica* have similar domain structure (containing only PX domain, but lacking BAR domain) and lipid-binding specificities, but showed distinct patterns of localisation and trogosome/phagosome recruitment, and phenotypes by gene silencing. We have shown by biochemical, genetic analyses and live imaging that EhSNX1, but not EhSNX2, is involved in the recruitment of EhVps26 during trogocytosis. We have also shown that EhSNX2 is negatively involved in trogocytosis per se, as demonstrated with partial augmentation of trogocytosis by *EhSNX2* gene silencing. Our data

indicate, together with our previous finding showing that EhVps26 of the retromer complex is recruited to the trogocytic cup (Nakada-Tsukui et al., 2005; Picazarri et al., 2015), that EhSNX1 recruits the retromer complex to the trogosome/phagosome in a PI3P-dependent manner. Unlike EhSNX1, EhSNX2 did not interact with the retromer complex as indicated. This result is consistent with the fact that the amino acid residues implicated for the binding with the retromer complex are not conserved in EhSNX2 (see Figure 2 and Section 2.2).

The fact that gene silencing of *EhSNX2*, but not *EhSNX1*, increased the trogocytosis efficiency was counter-intuitive and suggestive of *EhSNX2* being a negative regulator of trogocytosis. It has been shown that in dendritic cells, SNX3 overexpression causes defect in early endosome maturation by competing PI3P on early endosomes and reducing EEA1 recruitment (Chua & Wong, 2013). This observed phenotype may mirror the apparent upregulation of trogocytosis by *EhSNX2* gene silencing. However, the loss of competition for PI3P by *EhSNX2* gene silencing may not be the reason of the observed upregulation of trogocytosis because no change in trogocytosis was observed by *EhSNX1* gene silencing, which in theory also causes reduced competition for PI3P. The lack of phenotype by *EhSNX1* gene silencing may be explained at least in part by compensatory upregulation of *EhSNX2* gene expression by *EhSNX1* gene silencing. One possible scenario to explain these phenotypic changes in both human and *E. histolytica* is that both HsSNX3 and EhSNX2 employ a possible negative downstream effector/machinery needed for maturation of early endosomes and trogosomes.

### 3.4 | EhSNX1 binds to Arp2/3 complex for downstream signalling to cytoskeletal rearrangement during trogocytosis

We demonstrated that EhSNX1 specifically bound to ArpC3/ArpC4 of the Arp2/3 complex. ArpC3 and ArpC4 were found to interact with EhSNX1 as indicated by LC/MS/MS analysis of the immunoprecipitated samples using HA-EhSNX1 as a bait. In general, Arp2/3 complex is known to be composed of seven subunits and involved in elongation, branching, and cross-linking of actin filaments via regulation of actin nucleation and elongation (Goley & Welch, 2006). Because all components of the Arp2/3 complex were found in the previous phagosomal proteome analyses (Boettner et al., 2008; Furukawa, Nakada-tsukui, & Nozaki, 2013; Marion et al., 2005; Okada et al., 2006), the Arp2/3 complex was suggested to be involved in phagocytosis and trogocytosis. The recruitment of EhSNX1 to the trogocytosis initiation site was specific to EhSNX1 and not observed for EhSNX2. Precise timing of the recruitment of EhSNX1 to the trogocytosis initiation site relative to that of Arp2/3 was not determined as live imaging was unable to be performed. However, the recruitment of EhSNX1 appeared to slightly precede that of Arp2/3. The continuity of the association of EhSNX1 and Arp2/3 clearly indicates close and direct interplay between them, triggered by PI3P-dependent recruitment of EhSNX1 to the trogocytosis initiation site. It is worth noting that the localisation of EhVps26 and

EhArpC3 on the trogocytic cup were overlapping but not identical. Together with the observation that EhSNX1 partially colocalised with EhVps26, these observations indicate that EhSNX1 may play a role in the bridging cytoskeletal rearrangement by EhArpC3 and receptor recycling mediated by the retromer.

### 3.5 | The model proposed by EhSNX1/2 live imaging

Based on the biochemical, live imaging, and immunofluorescence image data, we propose the following model of how key players are engaged during trogocytosis (Figure 9). Upon the adherence of the amoebic trophozoite to the live mammalian cell, PI3P is locally synthesised in situ on the trogocytosis initiation site. EhSNX1 is recruited via PI3P binding mediated by its PX domain to the trogocytosis initiation site, which then becomes the trogocytic cup. EhSNX1 recruits Arp2/3 complex, which subsequently leads to actin cytoskeleton reorganisation needed for the establishment of the tunnel-like structure of the trogosomes and also the closure of trogosomes. At the same time, EhSNX1 also recruits the retromer complex via interaction with Vps26. The retromer complex then binds to the hydrolase receptors for the retrieval (and recycling) of the receptors. Once the trogocytic cup (or the trogosome) is enclosed, EhSNX2 is recruited to the trogosome by virtue of its PI3P-binding ability with a concomitant dissociation of EhSNX1. This model depicts a sequential involvement of EhSNX1 and EhSNX2 during the formation and maturation of trogosomes.

The apparent enhancement of trogocytosis by *EhSNX2* gene silencing is possibly due to the loss of negative feedback regulation toward the initial trogocytosis event(s) as explained above. However, its mechanism and the possible negative effector(s) remain elusive and need further investigation. The recruitment of EhSNX1 and 2 to the trogocytic cup and the trogosome was time- and localisation (domain)-specific. Although the underlying mechanism

of the spatiotemporal recruitment of EhSNXs remains unknown, it is plausible that phosphorylation of the conserved Ser72 (of HsSNX3; Figure S3) may regulate the binding of EhSNX1/2 to PI3P and other possible accessory and effector proteins in an isotype-specific manner.

The retromer complex was previously identified as an effector of GTP-bound active Rab7A in *E. histolytica* (Nakada-Tsukui et al., 2005). EhRab7A was reported to be localised to the preparatory vacuolar organelle that emerges upon erythrophagocytosis (pre-phagosomal vacuole), where EhRab7A and EhVps26 were colocalised. In this study, the effects of *EhSNX1* gene silencing on the inhibition of Vps26 recruitment to the trogosome was not large and rather marginal, suggesting that the recruitment of the retromer may be also regulated via EhRab7A.

## 4 | EXPERIMENTAL PROCEDURES

### 4.1 | Cells and reagents

Trophozoites of *E. histolytica* strains HM-1:IMSS cl6 (Diamond, Mattern, & Bartgis, 1972) and G3 (Bracha, Nuchamowitz, & Mirelman, 2003) were axenically cultured in BI-S-33 medium (BIS) at 35.5°C as previously described (Diamond et al., 1978). CHO cells were maintained in F-12 medium (Invitrogen-Gibco, Grand Island, NY) supplemented with 10% fetal bovine serum in 25 cm<sup>2</sup> tissue culture flasks (IWAKI, Shizuoka, Japan) under 5% CO<sub>2</sub> at 37°C. All chemicals of analytical grade were purchased from Sigma-Aldrich (Missouri, USA) unless otherwise stated. The anti-HA (11MO) and anti-myc (9E10) monoclonal antibodies were purchased from Covance (Princeton, NJ, USA). The anti-GFP antibody was purchased from Sigma-Aldrich. The production of rabbit polyclonal antibodies against EhCS1, EhCP-A5, EhVps26, and EhVps35 were previously

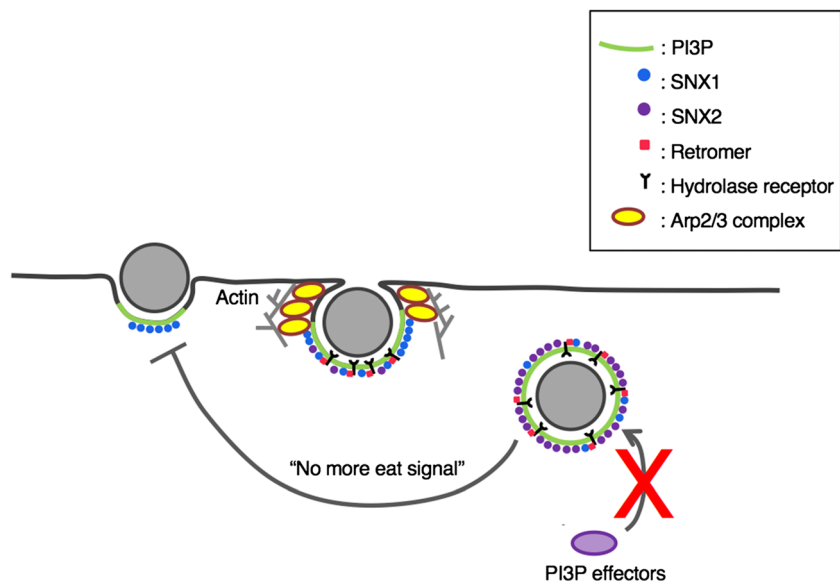


**FIGURE 9** A model of the involvement of PI3P, SNXs, the retromer, the hydrolase receptor, and Arp2/3 complex in phagocytosis/trogocytosis

described (Nakada-Tsukui et al., 2005; Nakada-Tsukui et al., 2009; Nozaki et al., 1999).

## 4.2 | Plasmid construction

Standard techniques were used for DNA manipulation, subcloning, and plasmid construction. Plasmid vectors to produce *E. histolytica* lines that express EhSNX1 (EHI\_060320) and EhSNX2 (EHI\_004400) with HA- or GFP-tag fused at the amino and carboxyl termini were constructed as follows. The full-length protein coding region of these genes was amplified by polymerase chain reaction (PCR) with following primers: 5'-GAACCCGGGATGGGAGATAATAAAGAAGATATTAT-3' and 5'-GAACTCGAGTTATTCTGATGATGATGAACTTTCAT-3' (*EhSNX1*) or 5'-GAACCCGGGATGAGTAATTATGCACAGTATGAATA-3' and 5'-GAACTCGAGTTACCAACTAGTAACCTCCCAATTGT-3' (*EhSNX2*), where the restriction enzyme sites are underlined. PCR-amplified fragments were digested by XmaI and XhoI and ligated into pEhEx-HA (Nakada-Tsukui et al., 2009) and pEhEx-GFP vectors (Somlata et al., 2017) that were predigested with the two enzymes and purified to construct the plasmid to produce HA-tagged and GFP-fused SNXs at the amino terminus. The resultant plasmids were designated as pEhExHA-SNX1, 2 and pEhExGFP-SNX1, 2, respectively. Note that pEhExGFP contains a linker corresponding to five repeats of GA dipeptides) after GFP. To construct plasmids to express EhSNX1 and EhSNX2 with HA tag at the carboxyl terminus, the full-length protein coding sequence of these genes was amplified by PCR with the following primers: 5'-GAAAGATCTATGGGAGATAATAAAGAAGATATTAT-3' and 5'-GAAAGATCTTTCTGATGATGATGAACTTTCATCAC-3' (*EhSNX1*); 5'-GAAAGATCTATGAGTAATTATGCACAGTATGAATA-3' and 5'-GAAAGATCTCCAAGTACTAGTAACCTCCCAATTGTCTT-3' (*EhSNX2*), where restriction enzyme sites are underlined. Amplified fragments were digested by BglII and ligated into pEhEx-HA. To construct plasmids for gene silencing of *EhSNX1* and *EhSNX2* gene, initial 420 bp of the *EhSNX1* coding region and full length (426 bp) of *EhSNX2* were PCR amplified with the following primers: 5'-GAAAGCCTATGGGAGATAATAAAGAAGATATTAT-3' and 5'-GAAAGACTCTTGACTTCTTAATGACTGAAATTGAG-3' (*EhSNX1*); 5'-GAAAGGCCTATGAGTAATTATGCACAGTATGAATA-3' and 5'-GAAGAGCTCTTACCAACTAGTAACCTCCCAATTGT-3' (*EhSNX2*). These PCR fragments were digested by StuI and SacI and ligated into StuI- and SacI-double digested psAP2-Gunma (Mi-ichi, Makiuchi, Furukawa, Sato, & Nozaki, 2011; Penuliar, Furukawa, Sato, & Nozaki, 2011). These plasmids were designated as psAP2-SNX1 and psAP2-SNX2. To construct vectors to express EhArpC3 with FLAG tag fused at the amino terminus, the full length protein coding sequence of these genes was amplified by PCR with the following primers: 5'-GAAACCCGGGATGACCACAATTGCCAACAAGATAA-3' and 5'-GAACTCGAGTTAAATGGTTTTGTTAAGAAGACTTTC-3' (*EhArpC3*), where restriction enzyme sites are underlined. Amplified fragments were digested by XmaI and XhoI, and ligated into pEhEx-FLAG, to produce pEhEx-FLAG-ArpC3. To express GFP-HrsFYVE with c-myc tag at the amino terminus under tetracycline induction in *E. histolytica*, a

plasmid was generated by subcloning the ORF of myc-GFP-HrsFYVE PCR-amplified from pKT-MG-Hrs-FYVE (Nakada-Tsukui, et al., 2009) to KpnI- and BamHI-double-digested pEhHygtetR-O-Cass vector, a kind gift from Dr. William A. Petri (Hamann, Buss, & Tannich, 1997; Ramakrishnan, Vines, Mann, & Petri, 1997) as previously described (Nakada-Tsukui et al., 2009).

## 4.3 | Establishment of *E. histolytica* transformants

The trophozoites of HM-1:IMSS cl6 were transfected with pEhExHA-SNX1, 2, pEhExGFP-SNX1, 2, pEhEx-FLAG-ArpC3, pEhExHA, pEhExGFP, and pEhExFLAG, whereas the trophozoites of G3 strain were transfected with psAP2-SNX1, psAP2-SNX2, and psAP2 by lipofection as previously described (Nozaki et al., 1999). Geneticin was added at a concentration of 1 µg/ml at 24 hr after transfection then gradually until the geneticin concentration reached 10 µg/ml.

## 4.4 | Immunoblot analysis

Approximately  $1 \times 10^5$  trophozoites were harvested in the exponential growth phase, washed twice with phosphate buffer saline (PBS), pH 7.4, and resuspended in 50 µl of lysis buffer (50-mM Tris-HCl, pH 7.5, 150-mM NaCl, 1% Triton X-100, containing 50 µg/ml of E-64, and complete mini). Approximately 20 µg of the total cell lysates were separated on 12% SDS-polyacrylamide gels and subsequently electrotransferred onto nitrocellulose membranes. The membranes were incubated with 5% non-fat dried milk in TBS-T (50-mM Tris-HCl, pH 8.0, 150-mM NaCl and 0.05% Tween-20) for 30 min. The proteins were reacted with primary mouse antibodies specific for HA (with the dilution of 1:1000), myc (1:1000), GFP (1:100), FLAG (1:1000) rabbit antisera against EhVps26 (1:100), EhVps35 (1:500), EhCP-A5 (1:1000), and CS1 (1:1000) at 4°C overnight. After the reaction with the primary antibodies, the membranes were washed with TBS-T three times; they were further reacted with horseradish peroxidase (HRP)-conjugated anti-mouse or anti-rabbit IgG antiserum (1:6000 or 1:8000, respectively) at room temperature for 1 hr. After washing with TBS-T three times, the specific proteins were visualised by chemiluminescence detection using Immobilon Western Chemiluminescent HRP Substrate (Millipore corporation, Massachusetts, USA) according to the manufacturer's protocol.

## 4.5 | Phagosome purification

Paramagnetic Dynabeads of 2.8-µm diameter (catalog number 14203; Invitrogen, California, USA) were incubated with human serum (Sigma-Aldrich) for 16 hr at 4°C, washed, and resuspended in transfection medium (OPTI-MEM I medium [Thermo Fisher, Massachusetts, USA], adjusted to pH 6.8, containing 5-mg/ml L-cysteine and 1-mg/ml ascorbic acid). Approximately  $2.4 \times 10^7$  trophozoites transferred to each well on six-well plates (Corning, New York, USA) and incubated at 35.5°C for 30 min to allow the trophozoites to attach to the surface of the well. After the medium was removed, a 2-ml transfection

medium containing approximately  $1 \times 10^7$  human serum-coated beads was added to each well (at the ratio 10 beads per cell). Beads were immediately sedimented on the surface of the amoebae seeded on the well by centrifugation at  $100 \times g$  at room temperature for 5 min. OPTI-MEM was removed and 3 ml of worm BIS was added. The plates were further incubated at  $35.5^\circ\text{C}$  for 30 min. After incubation, the medium was removed and 3 ml of cold PBS was added to each well of the plates. The plates were put on ice for 10 min to detach the amoebae, and the amoebae were washed twice with cold PBS. After centrifugation at  $800 \times g$  at  $4^\circ\text{C}$  for 3 min, the supernatant was removed and the amoebae were resuspended in 500  $\mu\text{l}$  of 8 mg/ml dithiobis (succinimidyl propionate; DSP) solution (Thermo Fisher, Massachusetts, USA), containing 0.5 mM of  $\beta$ -glycerophosphate, 0.1 mM of ethylenediaminetetraacetic acid (EDTA), 10-mM sodium fluoride, and 1-mM sodium orthovanadate. The mixture was incubated on the rotator (10 rpm) at  $4^\circ\text{C}$  for 30 min. To quench the reaction, 50  $\mu\text{l}$  of 1 M Tris-HCl, pH 7.5 was added and the mixture was further incubated as above for 10 min. After the amoebae were treated with DSP, they were washed with homogenisation buffer (250-mM sucrose, 3-mM imidazol, in PBS, pH 7.4, and complete mini [Sigma Aldrich]). Cells were mechanically disrupted by applying 25–70 strokes of Dounce homogeniser. The homogenate was centrifuged at  $800 \times g$  at  $4^\circ\text{C}$  for 3 min to remove unbroken cells. Bead-containing phagosomes were concentrated from the lysates by magnetic separation on PureProteome Magnetic Stand (Merck). The phagosomes were washed five times with 500  $\mu\text{l}$  of homogenisation buffer containing protease inhibitors and lysed with 50  $\mu\text{l}$  of lysis buffer (50-mM Tris-HCl, pH 7.5, 150-mM NaCl, 1% Triton X-100, containing 50  $\mu\text{g}/\text{ml}$  of E-64, and complete mini). For immunoblot analysis, approximately 20  $\mu\text{g}$  of phagosomes were resuspended in SDS-PAGE sample buffer (0.25-M Tris-HCl, pH 6.8, 8% SDS, 8% 2-mercaptoethanol, 40% Glycerol, 0.004% Bromophenol Blue), boiled for 5 min, and subjected to SDS-PAGE.

#### 4.6 | Lipid overlay assay

Approximately  $6 \times 10^6$  cells were harvested and washed with PBS. Approximately 150  $\mu\text{l}$  of lysis buffer (50-mM Tris-HCl, pH7.5, 15-mM NaCl, containing 1% Triton X-100, 0.05-mg/ml E-64, and complete mini) was added to an approximately 100- $\mu\text{l}$  bed volume of the pellet. The mixtures were incubated on ice for 30 min and centrifuged at  $16,000 \times g$  for 5 min. The supernatant was saved after centrifugation and used as the total lysate. Nitrocellulose membranes on which various phosphoinositides and other lipids had been spotted (PIP strips: P-6001, Echelon Biosciences, Salt Lake City, USA) were treated with 1% fatty acid-free bovine serum albumin (Sigma–Aldrich) in PBS-T (PBS containing 0.05% Tween 20) for 1 hr at room temperature for blocking. The membranes were incubated with 2 ml of the lipid-binding solution (PBS-T containing 1% fatty acid free bovine serum albumin and complete mini) containing 20-fold diluted amebic lysates for 2 hr at  $4^\circ\text{C}$ . After incubation with amoebic lysates, the membranes were washed with PBS-T three times at  $4^\circ\text{C}$ . The membranes were

then reacted with anti-HA (with the dilution of 1:500), anti-myc mouse monoclonal (1:500), anti-GFP mouse monoclonal (1:100) antibodies, anti-EhVps26 (1:100), and anti-EhVps35 rabbit antisera (1:500), at  $4^\circ\text{C}$  for 3 hr. After the membranes were washed twice with PBS-T at  $4^\circ\text{C}$ , they were further reacted with HRP-conjugated anti-mouse or anti-rabbit IgG antiserum (1:6000 or 1:8000, respectively) at  $4^\circ\text{C}$  for 1 hr. After washing three times with PBS-T at  $4^\circ\text{C}$ , the specific proteins were visualised by chemiluminescence detection using Immobilon Western Chemiluminescent HRP Substrate (Millipore corporation, Massachusetts, USA) according to the manufacturer's protocol.

#### 4.7 | Quantitative real-time PCR

The levels of *EhSNX1* and *EhSNX2* gene transcripts were analysed by quantitative real-time PCR. PolyA RNA was extracted, cDNA was prepared, and PCR was performed with cDNA as a template, as previously described (Mitra, Saito-Nakano, Nakada-Tsukui, Sato, & Nozaki, 2007). RNA polymerase II served as an internal control (GenBank accession number, XP\_649091; Gilchrist et al., 2006). PCR was performed using the following primer sets: sense primer, 5'-CCTGGTTATAGATTTAAACCAGAAATTTACTGAACA-3' and antisense primer, 5'-GAACTCGAGTTATTCTGATGATGATGAACCTTCAT-3' for *EhSNX1*; sense primer 5'-TCGG-TACAATCCCACCTCTCCCTGGAGATACAATC-3' and antisense primer 5'-GAACTCGAGTTACCAACTAGTAACTTCCCAATTGT-3' for *EhSNX2* and the following cycling parameters: an initial step of denaturation at  $95^\circ\text{C}$  for 20 s, followed by 40 cycles of denaturation at  $95^\circ\text{C}$  for 3 s, annealing and extension at  $60^\circ\text{C}$  for 30 s.

#### 4.8 | Staining of CHO cells

After CHO cells were cultured as described above on 10-cm diameter plastic dishes (IWAKI) for 2 days (before reaching confluence), they were incubated with CellTracker Blue CMAC Dye (Thermo Fisher) at the final concentration of 10  $\mu\text{M}$  at  $37^\circ\text{C}$  for 30 min. CHO cells were detached from the surface of the flasks by treating with PBS containing 0.5-mg/ml trypsin and 0.2-mM EDTA at  $37^\circ\text{C}$  for 5 min, washed twice with PBS, and resuspended in 600  $\mu\text{l}$  of transfection medium per  $3 \times 10^6$  CHO cells harvested from one dish.

#### 4.9 | Immunofluorescence assay

Approximately  $5 \times 10^3$  *E. histolytica* trophozoites were incubated with  $5 \times 10^4$  Dynabeads M-280 Tosylactivated beads (Invitrogen, California, USA) or  $5 \times 10^4$  CHO cells, which had been prestained with CellTracker Blue as described below, in 50- $\mu\text{l}$  BI-S-33 medium in 8-mm round wells on a slide glass at  $35.5^\circ\text{C}$  for 15 min. Cells were fixed with 3.7% paraformaldehyde and subsequently permeabilised with 0.2% saponin in PBS containing 1% bovine serum albumin for 10 min each at room temperature. The cells were reacted with anti-HA mouse antibody (with the dilution of 1:1000) or anti-Vps26 rabbit

antibody (1:1000) as previously described (Nakada-Tsukui et al., 2005). After washing with PBS three times, the cells were reacted with Alexa Fluor-488 anti-mouse secondary antibody (1:1000) or Alexa Fluor-568 anti-rabbit secondary antibody (1:1000; Thermo Fisher), respectively. The samples were observed using Carl-Zeiss LSM 780 Meta laser-scanning confocal microscope. The resultant images were further analysed using Zen software (Carl Zeiss, Oberkochen, Germany).

#### 4.10 | Live imaging and quantification of GFP-fused EhSNXs

Approximately  $7 \times 10^4$  trophozoites of the amoeba transformants transfected with pEhExGFP-SNX1, 2, or pEhExGFP were cultured on 3.5-cm diameter glass bottom dish in BIS medium under reduced oxygen using Anaerocult (Merck). After the medium was removed, approximately  $7 \times 10^5$  CHO cells were added to the dish at the ratio of 10 CHO cells per amoeba, and the center part of the glass bottom dish was covered by a cover slip. Live imaging was performed on Carl Zeiss LSM780 (Oberkochen, Germany) with default settings on the time series mode. Images captured were analysed by ZEN software (Carl Zeiss). The recruitment of GFP-EhSNX1/2 to phagosomes and trogosomes was estimated by quantitating the fluorescent intensity of a region of interest on the phagosome membrane and the neighboring cytoplasm. The average intensity per pixel of the region of interest was calculated. The ratio of the fluorescence intensity of GFP-EhSNX1/2 on the phagosome membrane against that in the cytosol was calculated and referred as the relative fluorescent signal on the membrane.

#### 4.11 | Cross-linking and immunoprecipitation of HA-tagged EhSNXs and native EhVps26

Approximately  $1 \times 10^6$  trophozoites of the amoeba transformants transfected with pEhExHA-SNX1, pEhExHA-SNX2, pEhExSNX1-HA, pEhExSNX2-HA, or pEhExHA were cultured on a 10-cm diameter dish in BIS medium with reduced oxygen using Anaerocult (Merck). CHO cells were added to the dish at the ratio of 10 CHO cells per amoeba, and the dish was incubated at 35.5°C for 30 min. After the medium containing uningested CHO cells was removed, the amoebae were detached from the surface of the dishes by adding cold PBS into the dishes and incubating them on ice for 10 min. After the trophozoites were washed with PBS three times, the cell pellet was cross-linked with DSP as described above. After washing twice with PBS, the cells were lysed with 800  $\mu$ l of lysis buffer (50-mM Tris-HCl, pH 7.5, 15-mM NaCl, containing 1% Triton X-100, 0.05 mg/ml E-64, and complete mini). After the debris was removed by centrifugation at 16,000  $\times$  g at 4°C for 5 min, the lysates were mixed and incubated with 50  $\mu$ l of protein G Sepharose beads (GE Healthcare, Illinois, USA; 80% slurry) at 4°C for 1 hr. After centrifugation at 800  $\times$  g at room temperature for 3 min, the supernatant was transferred to a new 1.5-ml microtube containing either approximately 50  $\mu$ l (80% slurry) of anti-HA monoclonal antibody produced in mouse, clone HA-7, purified immunoglobulin conjugated to agarose beads (Sigma-Aldrich) or 50  $\mu$ l of

protein G Sepharose (GE Healthcare), which was treated with 250  $\mu$ l of PBS, 2  $\mu$ l of anti-Vps26 rabbit antiserum for 1 hr at 4°C, was incubated with inversion at 4°C for 3.5 hr. The mixture was centrifuged at 800  $\times$  g to separate unbound proteins. The beads were washed three times with 1 ml of lysis buffer. After washing, the beads were resuspended in 180  $\mu$ l of lysis buffer containing HA-peptide at the final concentration of 0.2 mg/ml and the mixture was incubated at 4°C overnight to elute the bound proteins for HA-EhSNXs or directly boiled with 50  $\mu$ l of 2 $\times$  SDS-PAGE sample buffer for EhVps26.

#### 4.12 | Quantification of trogocytosis and phagocytosis using image cytometer

Approximately  $3 \times 10^5$  trophozoites were incubated in 6 ml of BIS medium containing 10- $\mu$ M CellTracker Green for 30 min at 35.5°C. CHO cells were stained with 10- $\mu$ M CellTracker Blue as described above. Approximately  $1 \times 10^5$  trophozoites were seeded onto a 3.5-cm diameter glass bottom dish in 2 ml of BIS medium and incubated for 20 min. For trogocytosis measurement, after removing the supernatant, approximately  $1 \times 10^5$  CHO cells in 90- $\mu$ l BIS medium were added onto the 1.0-cm diameter glass central pit of the dish. For phagocytosis measurement, CHO cells were killed by incubating at 55°C for 15 min and added to the pit of the dish. After the pit was covered with a cover glass, the mixture was cultivated at 35.5°C under anaerobic conditions. The images were taken on a Confocal Quantitative Image Cytometer, CQ1 (Yokogawa Electric Corporation, Tokyo, Japan) every 10 min for 80 min. The volume of the ingested CHO cells (blue) was calculated using three-dimensionally reconstituted data. The data shown are the average of the volumes of all trogosomes per amoeba in three wells each. Amoebae were mixed with CHO cells prepared as described above, and images were captured on CQ1. To analyse these data using three-dimensional structured images, CQ1 was set as below. At first, the top and bottom positions of a Z-stack contain almost all phagosomes. The number of slices depends on the distance between layers, which should be less than 4  $\mu$ m. The images were further analysed to quantify the volume and the fluorescence intensity of the ingested CHO cells using the CellPathfinder high content analysis software from the manufacturer of CQ1.

#### CONFLICT OF INTEREST

The authors declare no conflict of interest.

#### FUNDING INFORMATION

Grants-in-Aid for Scientific Research (B) and Challenging Research (Exploratory) (KAKENHI JP26293093, JP17K19416, and JP18H02650 to T.N.) and Grants-in-Aid for Scientific Research (B) and (C) (JP16K08766 and JP19H03463 to K.N.-T.) from the Japan Society for the Promotion of Science.

Grant for research on emerging and re-emerging infectious diseases from Japan Agency for Medical Research and Development (AMED, JP18fk0108046 to T.N.; 17fk0108122j1101, 18fk0108049j1102, and 19fk0108049j1103 to K.N.-T)

Grant for US-Japan Cooperative Medical Science Program from AMED (JP17jk0210018 to K.N.-T.)

Grant from the National Center for Global Health and Medicine Intramural Research Fund (29–2013 to T.N.)

Grant for Science and Technology Research Partnership for Sustainable Development (SATREPS) from AMED and Japan International Cooperation Agency (JICA) (T.N.).

## ORCID

Kumiko Nakada-Tsukui  <https://orcid.org/0000-0001-9832-916X>

Tomoyoshi Nozaki  <https://orcid.org/0000-0003-1354-5133>

## REFERENCES

- Boettner, D. R., Huston, C. D., Linford, A. S., Buss, S. N., Hout, E., Sherman, N. E., & Petri, W. A. (2008). *Entamoeba histolytica* phagocytosis of human erythrocytes involves PATMK, a member of the transmembrane kinase family. *PLoS Pathogens*, 4, 122–133. <https://doi.org/10.1371/journal.ppat.0040008>
- Bonifacino, J. S., & Hurley, J. H. (2008). Retromer. *Current Opinion in Cell Biology*, 20, 427–436. <https://doi.org/10.1016/j.ceb.2008.03.009>
- Bracha, R., Nuchamowitz, Y., & Mirelman, D. (2003). Transcriptional silencing of an amoebapore gene in *Entamoeba histolytica*: Molecular analysis and effect on pathogenicity. *Eukaryotic Cell*, 2, 295–305. <https://doi.org/10.1128/EC.2.2.295-305.2003>
- Burman, C., & Ktistakis, N. T. (2010). Regulation of autophagy by phosphatidylinositol 3-phosphate. *FEBS Letters*, 584, 1302–1312. <https://doi.org/10.1016/j.febslet.2010.01.011>
- Byekova, Y. A., Powell, R. R., Welter, B. H., & Temesvari, L. A. (2010). Localization of phosphatidylinositol (3,4,5)-trisphosphate to phagosomes in *Entamoeba histolytica* achieved using glutathione S-transferase- and green fluorescent protein-tagged lipid biosensors. *Infection and Immunity*, 78, 125–137. <https://doi.org/10.1128/IAI.00719-09>
- Chua, R. Y. R., & Wong, S. H. (2013). SNX3 recruits to phagosomes and negatively regulates phagocytosis in dendritic cells. *Immunology*, 139(1), 30–47. <https://doi.org/10.1111/imm.12051>
- Cullen, P. (2008). Endosomal sorting and signalling: An emerging role for sorting nexins. *Nature Reviews Molecular Cell Biology*, 9, 574–582. <http://www.nature.com/nrm/journal/v9/n7/abs/nrm2427.html>; jsessionid=2B6040A2FF75C8EA809BE493E30C2D52, <https://doi.org/10.1038/nrm2427>
- Diamond, L. S., Mattern, C. F. T., & Bartgis, I. L. (1972). Viruses of *Entamoeba histolytica*. I. Identification of transmissible virus-like agents. *Journal of Virology*, 9, 326–341.
- Diamond, L. S., Harlow, D. R., & Cunnik, C. C., (1978). A new medium for the axenic cultivation of *Entamoeba histolytica* and other *Entamoeba*. *Trans R Soc Trop Med Hyg*, 72, 431–432.
- Furukawa, A., Nakada-Tsukui, K., & Nozaki, T. (2013). Cysteine protease-binding protein family 6 mediates the trafficking of amylases to phagosomes in the enteric protozoan *Entamoeba histolytica*. *Infection and Immunity*, 81, 1820–1829. <https://doi.org/10.1128/IAI.00915-12>
- Gilchrist, C. A., Hout, E., Trapaidze, N., Fei, Z., Crasta, O., Asgharpour, A., ... Petri, W. A. (2006). Impact of intestinal colonization and invasion on the *Entamoeba histolytica* transcriptome. *Molecular and Biochemical Parasitology*, 147, 163–176. <https://doi.org/10.1016/j.molbiopara.2006.02.007>
- Goley, E. D., & Welch, M. D. (2006). The ARP2/3 complex: An actin nucleator comes of age. *Nature Reviews Molecular Cell Biology*, 7, 713–726. <https://doi.org/10.1038/nrm2026>
- Hamann, L., Buss, H., & Tannich, E., (1997). Tetracycline controlled gene expression in *Entamoeba histolytica*. *MolBiochem Parasitol*, 84, 83–91.
- Lenoir, M., Ustunel, C., Rajesh, S., Kaur, J., Moreau, D., Gruenberg, J., & Overduin, M. (2018). Phosphorylation of conserved phosphoinositide binding pocket regulates sorting nexin membrane targeting. *Nature Communications*, 9, 1–12. <https://doi.org/10.1038/s41467-018-03370-1>
- Lozano, R., Naghavi, M., Foreman, K., Lim, S., Shibuya, K., Aboyans, V., ... Murray, C. J. L. (2012). Global and regional mortality from 235 causes of death for 20 age groups in 1990 and 2010: A systematic analysis for the Global Burden of Disease Study 2010. *The Lancet*, 380, 2095–2128. [https://doi.org/10.1016/S0140-6736\(12\)61728-0](https://doi.org/10.1016/S0140-6736(12)61728-0)
- Marion, S., Laurent, C., & Guillén, N. (2005). Signalization and cytoskeleton activity through myosin IB during the early steps of phagocytosis in *Entamoeba histolytica*: a proteomic approach. *Cellular Microbiology*, 7, 1504–1518. <https://doi.org/10.1111/j.1462-5822.2005.00573.x>
- Meng, X., & Ji, Y. (2013). Modern computational techniques for the HMMER sequence analysis. *ISRN Bioinformatics*, 2013, 1–13. <https://doi.org/10.1155/2013/252183>
- Mi-ichi, F., Makiuchi, T., Furukawa, A., Sato, D., & Nozaki, T. (2011). Sulfate activation in mitochondria plays an important role in the proliferation of *Entamoeba histolytica*. *PLoS Neglected Tropical Diseases*, 5, 1–7. <https://doi.org/10.1371/journal.pntd.0001263>
- Mitra, B. N., Saito-Nakano, Y., Nakada-Tsukui, K., Sato, D., & Nozaki, T. (2007). Rab11B small GTPase regulates secretion of cysteine proteases in the enteric protozoan parasite *Entamoeba histolytica*. *Cellular Microbiology*, 9, 2112–2125. <https://doi.org/10.1111/j.1462-5822.2007.00941.x>
- Nakada-Tsukui, K., Okada, H., Mitra, B. N., & Nozaki, T. (2009). Phosphatidylinositol-phosphates mediate cytoskeletal reorganization during phagocytosis via a unique modular protein consisting of RhoGEF/DH and FYVE domains in the parasitic protozoan *Entamoeba histolytica*. *Cellular Microbiology*, 11, 1471–1491. <https://doi.org/10.1111/j.1462-5822.2009.01341.x>
- Nakada-Tsukui, K., Saito-nakano, Y., Ali, V., & Nozaki, T. (2005). A retromerlike complex is a novel Rab7 effector that is involved in the transport of the virulence factor cysteine protease in the enteric protozoan parasite *Entamoeba histolytica*. *Molecular Biology of the Cell*, 16, 5294–5303. <https://doi.org/10.1091/mbc.E05>
- Nozaki, T., Asai, T., Sanchez, L. B., Kobayashi, S., Nakazawa, M., & Takeuchi, T. (1999). Characterization of the gene encoding serine acetyltransferase, a regulated enzyme of cysteine biosynthesis from the protist parasites *Entamoeba histolytica* and *Entamoeba dispar*: Regulation and possible function of the cysteine biosynthetic pathway in *Entamoeba*. *Journal of Biological Chemistry*, 274, 32445–32452. <https://doi.org/10.1074/jbc.274.45.32445>
- Okada, M., Huston, C. D., Oue, M., Mann, B. J., Petri, W. A., Kita, K., & Nozaki, T. (2006). Kinetics and strain variation of phagosome proteins of *Entamoeba histolytica* by proteomic analysis. *Molecular and Biochemical Parasitology*, 145, 171–183. <https://doi.org/10.1016/j.molbiopara.2005.10.001>
- Penuliar, G. M., Furukawa, A., Sato, D., & Nozaki, T. (2011). Mechanism of trifluoromethionine resistance in *Entamoeba histolytica*. *Journal of Antimicrobial Chemotherapy*, 66, 2045–2052. <https://doi.org/10.1093/jac/dkr238>
- Picazari, K., Nakada-Tsukui, K., Tsuboi, K., Miyamoto, E., Watanabe, N., Kawakami, E., & Nozaki, T. (2015). Atg8 is involved in endosomal and phagosomal acidification in the parasitic protist *Entamoeba histolytica*. *Cellular Microbiology*, 17, 1510–1522. <https://doi.org/10.1111/cmi.12453>
- Ralston, K. S. (2015). Taking a bite: Amoebic trophocytosis in *Entamoeba histolytica* and beyond. *Current Opinion in Microbiology*, 28, 26–35. <https://doi.org/10.1016/j.mib.2015.07.009>
- Ralston, K. S., Solga, M. D., MacKey-Lawrence, N. M., Bhattacharya, A., & Petri, W. A. (2014). Trophocytosis by *Entamoeba histolytica* contributes

- to cell killing and tissue invasion. *Nature*, 508, 526–530. <https://doi.org/10.1038/nature13242>
- Ramakrishnan, G., Vines, R. R., Mann, B. J., & Petri, W. A., Jr. (1997). A tetracycline-inducible gene expression system in *Entamoeba histolytica*. *Mol Biochem Parasitol*, 84, 93–100.
- Seaman, M. N. J. (2012). The retromer complex—Endosomal protein recycling and beyond. *Journal of Cell Science*, 125, 4693–4702. <https://doi.org/10.1242/jcs.103440>
- Somlata, Nakada-Tsukui, K., & Nozaki, T. (2017). AGC family kinase 1 participates in trogocytosis but not in phagocytosis in *Entamoeba histolytica*. *Nature Communications*, 8, 1–12. <https://doi.org/10.1038/s41467-017-00199-y>
- Srivastava, V. K., Yadav, R., Watanabe, N., Tomar, P., Mukherjee, M., Gourinath, S., ... Datta, S. (2017). Structural and thermodynamic characterization of metal binding in Vps29 from *Entamoeba histolytica*: Implication in retromer function. *Molecular Microbiology*, 106, 562–581. <https://doi.org/10.1111/mmi.13836>
- Worby, C. A., & Dixon, J. E. (2002). Sorting out the cellular functions of sorting nexins. *Nature Reviews. Molecular and Cellular Biology*, 3, 919–931.
- Yeung, T., & Sergio, G. (2007). Lipid signaling and the modulation of surface charge during phagocytosis. *Immunological Reviews*, 219, 17–36. <https://doi.org/10.1111/j.1600-065X.2007.00546.x>
- Yousuf, M. A., Mi-Ichi, F., Nakada-Tsukui, K., & Nozaki, T. (2010). Localization and targeting of an unusual pyridine nucleotide transhydrogenase in *Entamoeba histolytica*. *Eukaryotic Cell*, 9, 926–933. <https://doi.org/10.1128/EC.00011-10>

## SUPPORTING INFORMATION

Additional supporting information may be found online in the Supporting Information section at the end of the article.

**How to cite this article:** Watanabe N, Nakada-Tsukui K, Nozaki T. Two isoforms of phosphatidylinositol 3-phosphate-binding sorting nexins play distinct roles in trogocytosis in *Entamoeba histolytica*. *Cellular Microbiology*. 2020;22:e13144. <https://doi.org/10.1111/cmi.13144>